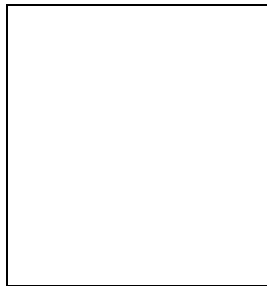


MEASUREMENTS FROM KTeV OF RARE DECAYS OF THE K_L^0 AND π^0

E. D. ZIMMERMAN
University of Colorado
Boulder, Colorado 80302 USA



The KTeV collaboration at Fermi National Accelerator Laboratory has recently completed searches for and measurements of several decay modes of the neutral kaon and pion. These include new searches for lepton flavor violating decays (which have not been seen), and a new study of the parity properties of the decay $\pi^0 \rightarrow e^+e^-e^+e^-$.

1 The KTeV Detector

Fermilab's KTeV detector (Fig. 1) was constructed for Experiments 799 and 832. The two experiments were designed to concentrate on different aspects of neutral kaon physics: E799 on rare decays of the K_L and E832 on measurement of $\text{Re}(\epsilon'/\epsilon)$. A primary proton beam with energy 800 GeV struck a BeO target at a targeting angle of 4.8 mrad, and collimation and sweeping magnets produced two parallel neutral hadron beams. The beams entered a 60 m long vacuum decay region, which ended at a Mylar-Kevlar vacuum window. Decay products were tracked with a series of drift chambers surrounding a dipole analysis magnet. Downstream of the drift chambers were a series of transition radiation detectors (TRD) (in E799 only) and a pure CsI electromagnetic calorimeter, an active hadron beam absorber, and a set of muon detectors behind steel shielding. Photon veto detectors surrounded the fiducial volume in the transverse directions. The detector is described in more detail in Ref. ¹.

2 The decay $\pi^0 \rightarrow e^+e^-e^+e^-$ and the parity of the π^0

The neutral pion's parity has historically been studied in two ways: indirectly via the cross-section of π^- capture on deuterons^{2,3}, or directly via the double Dalitz decay $\pi^0 \rightarrow e^+e^-e^+e^-$ ⁴. While both sets of results are consistent with the negative parity, the direct measurement has only 3.6 σ significance. KTeV has now reported results⁵ that conclusively confirm the negative π^0

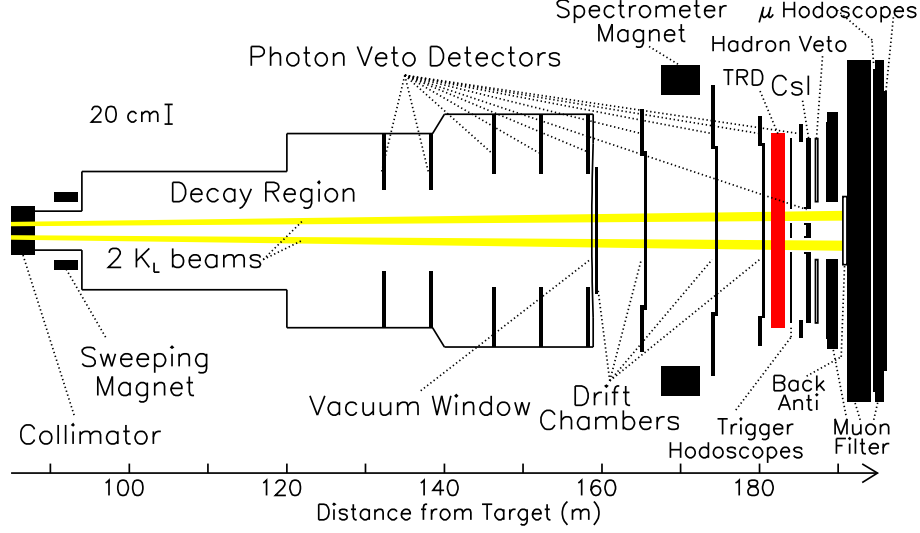


Figure 1: The KTeV spectrometer as configured for E799.

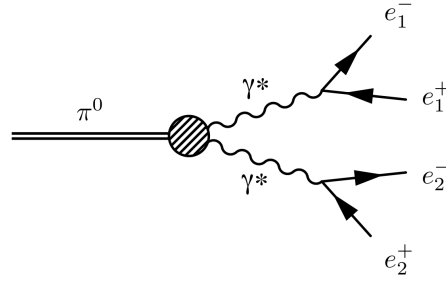


Figure 2: Lowest order Feynman diagram for $\pi^0 \rightarrow e^+e^-e^+e^-$. The direct contribution is shown; a second diagram exists with e_1^+ and e_2^+ exchanged.

parity as well as the first-ever searches for parity and CPT violation, and the first measurements of the electromagnetic form factor, in this mode.

The $\pi^0 \rightarrow e^+e^-e^+e^-$ decay proceeds through a two-photon intermediate state (Fig. 2). The most general interaction Lagrangian for the $\pi^0 \rightarrow \gamma^*\gamma^*$ transition can be written⁶:

$$\mathcal{L} \propto C_{\mu\nu\rho\sigma} F^{\mu\nu} F^{\rho\sigma} \Phi \quad (1)$$

where $F^{\mu\nu}$ and $F^{\rho\sigma}$ are the photon fields, Φ is the pion field, and the coupling has the form

$$C_{\mu\nu\rho\sigma} \propto f(x_1, x_2) [\cos \zeta \epsilon_{\mu\nu\rho\sigma} + \sin \zeta e^{i\delta} (g_{\mu\rho} g_{\nu\sigma} - g_{\mu\sigma} g_{\nu\rho})]. \quad (2)$$

The first term in $C_{\mu\nu\rho\sigma}$ is the expected pseudoscalar coupling and the second term introduces a scalar coupling with a mixing angle ζ and a phase difference δ . Nuclear parity violation would introduce a nonzero ζ , while CPT violation would cause the phase δ to be nonzero. We assume the standard parity-conserving form for the $\gamma^* \rightarrow e^+e^-$ conversion.

The form factor $f(x_1, x_2)$ is expressed in terms of the momentum transfer of each of the virtual photons, or equivalently the invariant masses of the two Dalitz pairs: $x_1 \equiv (m_{e_1^+e_1^-}/M_{\pi^0})^2$; $x_2 \equiv (m_{e_2^+e_2^-}/M_{\pi^0})^2$. In calculating the phase space variables for an individual event, there is an intrinsic ambiguity in assigning each electron to a positron to form a Dalitz pair. KTeV's analysis uses a matrix element model that includes the exchange diagrams and therefore avoids

the need to enforce a pairing choice. The form factor is parametrized using a model based on that of D’Ambrosio, Isidori, and Portolés (DIP)⁷, but with an additional constraint that ensures the coupling vanishes at large momenta⁸. In terms of the remaining free parameters, the form factor is:

$$f_{\text{DIP}}(x_1, x_2; \alpha) = \frac{1 - \mu(1 + \alpha)(x_1 + x_2)}{(1 - \mu x_1)(1 - \mu x_2)}, \quad (3)$$

where $\mu = M_{\pi^0}^2/M_\rho^2 \approx 0.032$.

The parity properties of the decay can be extracted from the angle ϕ between the planes of the two Dalitz pairs in Fig. 2, where pair 1 is defined as having the smaller invariant mass. The distribution of this angle from the dominant direct contribution has the form $d\Gamma/d\phi \sim 1 - A \cos(2\phi) + B \sin(2\phi)$, where $A \approx 0.2 \cos(2\zeta)$ and $B \approx 0.2 \sin(2\zeta) \cos \delta$. A pure pseudoscalar coupling, therefore, would produce a negative $\cos(2\phi)$ dependence.

The branching ratio measurement, which we describe here first, makes use of a normalization mode in which two pions decay via $\pi^0 \rightarrow e^+e^-\gamma$ and the third $\pi^0 \rightarrow \gamma\gamma$. This “double single-Dalitz” mode, denoted $K_L \rightarrow \pi^0\pi_D^0\pi_D^0$ where π_D^0 refers to $\pi^0 \rightarrow e^+e^-\gamma$, has the same final state particles as the signal mode. Both modes are fully reconstructed in the detector and the total invariant mass is required to match the kaon’s. The two modes are distinguished by a χ^2 formed of the three reconstructed π^0 masses. This serves to identify the best pairing of particles for a given decay hypothesis, as well as to select the more likely hypothesis of the two. The similarity of these modes allows cancellation of most detector-related systematic effects in the branching ratio measurement, but also allows each mode to be a background to the other.

Radiative corrections complicate the definition of the Dalitz decays in general. We define the signal mode $\pi^0 \rightarrow e^+e^-e^+e^-$ to be inclusive of radiative final states where the squared ratio of the invariant mass of the four electrons to the neutral pion mass $x_{4e} \equiv (M_{4e}/M_{\pi^0})^2$ is greater than 0.9, while events with $x_{4e} < 0.9$ (approximately 6% of the total rate) are treated as $\pi^0 \rightarrow e^+e^-e^+e^-\gamma$. For normalization, the decay $\pi^0 \rightarrow e^+e^-\gamma$ is understood to include all radiative final states, for consistency with previous measurements of this decay⁹. Radiative corrections in this analysis are taken from an analytic calculation to order $\mathcal{O}(\alpha^2)$ ⁶.

Radiative corrections complicate the definition of the Dalitz decays in general. The signal mode $\pi^0 \rightarrow e^+e^-e^+e^-$ is defined to be inclusive of radiative final states where the squared ratio of the invariant mass of the four electrons to the neutral pion mass $x_{4e} \equiv (M_{4e}/M_{\pi^0})^2$ is greater than 0.9, while events with $x_{4e} < 0.9$ (approximately 6% of the total rate) are treated as $\pi^0 \rightarrow e^+e^-e^+e^-\gamma$. Radiative corrections in this analysis are taken from an analytic calculation to order $\mathcal{O}(\alpha^2)$ ⁶.

The final event sample contains 30 511 signal candidates with 0.6% residual background and 141 251 normalization mode candidates with 0.5% background (determined from the Monte Carlo simulation). The background in the signal sample is dominated by mistagged events from the normalization mode. v KTeV finds the following the ratio of decay rates:

$$\frac{B_{eeee}^{x>0.9} \cdot B_{\gamma\gamma}}{B_{ee\gamma}^2} = 0.2245 \pm 0.0014(\text{stat}) \pm 0.0009(\text{syst}). \quad (4)$$

The $\pi^0 \rightarrow e^+e^-e^+e^-$ branching ratio can be calculated from the double ratio using the known values $B_{\gamma\gamma} = 0.9980 \pm 0.0003$ and $B_{ee\gamma} = (1.198 \pm 0.032) \times 10^{-2}$ ¹⁰. This yields $B_{eeee}^{x>0.9} = (3.26 \pm 0.18) \times 10^{-5}$, where the error is dominated by the uncertainty in the $\pi^0 \rightarrow e^+e^-\gamma$ branching ratio. KTeV uses the radiative corrections model⁶ to extrapolate to all radiative final states, finding:

$$\frac{B_{eeee(\gamma)} \cdot B_{\gamma\gamma}}{B_{ee\gamma}^2} = 0.2383 \pm 0.0015(\text{stat}) \pm 0.0010(\text{syst}), \quad (5)$$

and $B_{eeee(\gamma)} = (3.46 \pm 0.19) \times 10^{-5}$. This branching ratio result is in good agreement with previous measurements⁴.

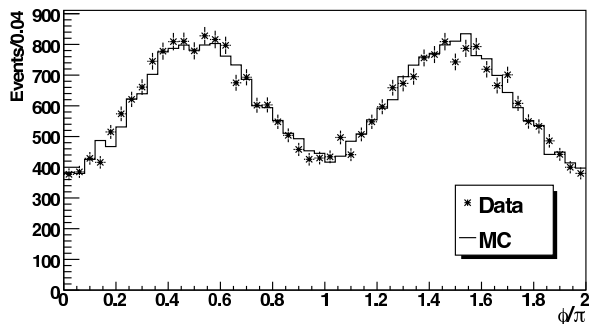


Figure 3: Distribution of the angle ϕ , in units of π , between the planes of the two e^+e^- pairs for $\pi^0 \rightarrow e^+e^-e^+e^-$ candidate decays. The solid histogram shows the Monte Carlo expectation for negative parity.

The parameters of the $\pi^0\gamma^*\gamma^*$ coupling are found by maximizing an unbinned likelihood function composed of the differential decay rate in terms of ten phase-space variables. The first five are $(x_1, x_2, y_1, y_2, \phi)$, where x_1 , x_2 , and ϕ are described above and the remaining variables y_1 and y_2 describe the energy asymmetry between the electrons in each Dalitz pair in the π^0 center of mass⁶. The remaining five are the same variables, but calculated with the opposite choice of e^+e^- pairings. The likelihood is calculated from the full matrix element including the exchange diagrams and $\mathcal{O}(\alpha^2)$ radiative corrections.

The fit yields the DIP α parameter and the (complex) ratio of the scalar to the pseudoscalar coupling. For reasons of fit performance, the parity properties are fit to the equivalent parameters κ and η , where $\kappa + i\eta \equiv \tan \zeta e^{i\delta}$. The shape of the minimum of the likelihood function indicates that the three parameters α , κ , and η are uncorrelated. Acceptance-dependent effects are included as a normalization factor calculated from Monte Carlo simulations.

Systematic error sources on α and κ are similar to those for the branching ratio measurement. The dominant systematic error is due to variation of cuts, resulting in a total systematic error of 0.9 and 0.011 on α and κ respectively. For the η parameter, the primary uncertainty results from the resolution on the angle ϕ between the two lepton pairs. This behavior was studied with Monte Carlo simulation and a correction was calculated. The uncertainty on this correction results in a systematic error of 0.031.

The ϕ distribution is shown in Fig. 3. For plotting the data a unique pairing of the four electrons is chosen such that $x_1 < x_2$ and the product x_1x_2 is minimized: this choice represents the dominant contribution to the matrix element. It is clear that the pseudoscalar coupling dominates, as expected, with no evidence for a scalar component. The distributions of all five phase space variables agree well with the Monte Carlo simulation.

The parameters κ and η are transformed into limits on the pseudoscalar-scalar mixing angle ζ under two hypotheses. If CPT violation is allowed, then the limit is set by the uncertainties in η , resulting in $\zeta < 6.9^\circ$ at the 90% confidence level. If instead, CPT conservation is enforced, η must be zero, and the limit derives from the uncertainties on κ , resulting in $\zeta < 1.9^\circ$, at the same confidence level. These limits on ζ limit the magnitude of the scalar component of the decay amplitude, relative to the pseudoscalar component, to less than 12.1% in the presence of CPT violation, and less than 3.3% if CPT is assumed conserved. The limits on scalar contributions apply to all π^0 decays with two-photon intermediate or final states.

This analysis confirms the negative parity of the neutral pion with much higher statistical significance than the previous result, and places tight limits on nonstandard scalar and CPT -violating contributions to the $\pi^0 \rightarrow e^+e^-e^+e^-$ decay.

3 Lepton Flavor Violation

Lepton Flavor Violation (LFV) in weak decays is a key signature of several beyond-Standard Model physics scenarios. Supersymmetry¹¹, new massive gauge bosons^{12,13}, and technicolor¹⁴ all can lead to LFV decays which might be within reach of current experiments. Searches in K_L decays are complementary to searches in the charged lepton sector, since K_L decays probe the $s \rightarrow d\mu e$ transition¹². KTeV-E799 has searched for the decays $K_L \rightarrow \pi^0 \mu^\pm e^\mp$ and $\pi^0 \rightarrow \mu^\pm e^\mp$, and has made the first reported search for $K_L \rightarrow \pi^0 \pi^0 \mu^\pm e^\mp$ ¹⁵.

In each case, the analysis required two charged tracks, one of which was identified as a muon and the other an electron. The key detector elements for particle identification were E/p in the CsI calorimeter, response of the TRD, and muon hodoscopes downstream of the muon filter steel. Clusters in the CsI with no tracks pointing to them were considered photons.

3.1 $K_L \rightarrow \pi^0 \mu^\pm e^\mp$

The dominant background for $K_L \rightarrow \pi^0 \mu^\pm e^\mp$ was the decay $K_L \rightarrow \pi^\pm e^\mp \nu_e$ (K_{e3}), with a π^\pm decay or punch through to the muon hodoscopes, accompanied by two accidental photons faking a π^0 . Since accidental photons were often accompanied by other accidental activity, we removed events with evidence of additional in-time activity in the detector. Additionally, the two photons were required to form a good π^0 mass, and the square of the π^0 momentum in the K_L rest frame was required to be positive and therefore physical.

The signal and control regions were defined using a likelihood variable \mathbf{L} derived from p_t^2 , the sum of the momentum components of all final-state particles perpendicular to the kaon flight line, and $M_{\pi^0 \mu e}$, the invariant mass of the $\pi^0 \mu e$ system. The signal (control) region was defined by a cut on \mathbf{L} chosen to retain 95% (99%) of signal Monte Carlo events after all other cuts. Expected background levels were 0.66 ± 0.23 events in the signal region and 4.21 ± 0.53 events in the control region. Both the signal and control regions were blind during the analysis. Figure 4 shows the $p_t^2 - M_{\pi^0 \mu e}$ plane after all cuts: five events were found in the control region and zero in the signal. The resulting limit is $B(K_L \rightarrow \pi^0 \mu^\pm e^\mp) < 7.56 \times 10^{-11}$ at 90% CL, a factor of 82 improvement over the previous best limit for this mode.¹⁶

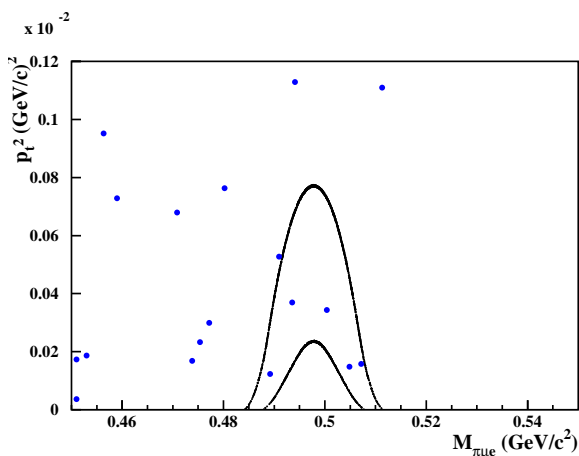


Figure 4: Surviving events in the $p_t^2 - M_{\pi^0 \mu e}$ plane for the $K_L \rightarrow \pi^0 \mu^\pm e^\mp$ search data. The signal and control regions are shown as the inner and outer solid contours.

3.2 Other lepton flavor violating modes

KTeV has also searched for the decay $K_L \rightarrow \pi^0 \pi^0 \mu^\pm e^\mp$. Reconstructing a second π^0 greatly reduces the backgrounds, so some particle identification and anti-accidental cuts were relaxed to improve the signal acceptance. A similar analysis, including a cut on a kinematic likelihood variable, yielded no events in either the control region or the signal region. This resulted in a limit $B(K_L \rightarrow \pi^0 \pi^0 \mu^\pm e^\mp) < 1.64 \times 10^{-10}$. This is the first limit reported for this decay.

The decay chain $K_L \rightarrow \pi^0 \pi^0 \pi^0$, $\pi^0 \rightarrow \mu^\pm e^\mp$ gives the same final state particles as $K_L \rightarrow \pi^0 \pi^0 \mu^\pm e^\mp$, and therefore the same analysis procedure applies with the additional requirement that the invariant mass $M_{\mu e} \approx M_{\pi^0}$. Since no events were found, the limit is $B(\pi^0 \rightarrow \mu^\pm e^\mp) < 3.59 \times 10^{-10}$. This limit on $\pi^0 \rightarrow \mu^\pm e^\mp$ is equally sensitive to both charge modes, while the previous best limits were not¹⁷. Assuming equal contributions from both charge combinations, KTeV's result is about a factor of two better than the previous best limit on $\pi^0 \rightarrow \mu^+ e^-$ and about a factor of 10 greater than the previous best limit on $\pi^0 \rightarrow \mu^- e^+$.

4 Conclusion

KTeV has completed several measurements recently on the decays of neutral K and π mesons. The measurement of $\pi^0 \rightarrow e^+ e^- e^+ e^-$ represents the best direct determination of the parity of the π^0 and the first searches for nonstandard parity and CPT violation in this mode. It also yields the best branching ratio and the first measurement of the form factor in this mode. The limits on lepton flavor violation are now the most stringent in the world for these decay modes.

Acknowledgments

KTeV acknowledges the support and effort of the Fermilab staff and the technical staffs of the institutions. This work was supported in part by the U.S. DOE, NSF, Ministry of Education and Science of Japan, Fundao de Amparo a Pesquisa do Estado de S Paulo-FAPESP, Conselho Nacional de Desenvolvimento Cientifico e Tecnologico-CNPq and CAPES-Ministerio Educao.

References

1. E. Abouzaid *et al.*, *Phys. Rev. D* **75**, 012004 (2007).
2. W. K. H. Panofsky, R. L. Aamodt, and J. Hadley, *Phys. Rev.* **81**, 565 (1951).
3. W. Chinowsky and J. Steinberger, *Phys. Rev.* **95**, 1561 (1954).
4. N. Samios *et al.*, *Phys. Rev.* **126**, 1844 (1962).
5. E. Abouzaid *et al.*, *Phys. Rev. Lett.* **100**, 182001 (2008).
6. A. R. Barker, H. Huang, P. A. Toale, and J. Engle, *Phys. Rev. D* **67**, 033008 (2003).
7. G. D'Ambrosio, G. Isidori, and J. Portolés, *PLB* **423**, 385 (1998).
8. P. A. Toale, PhD Thesis, The University of Colorado at Boulder (2004).
9. M. A. Schardt *et al.*, *PRD* **23**, 639 (1981).
10. W.-M. Yao *et al.*, *J. Phys. G* **33** 1 (2006).
11. A. Belyaev *et al.*, *Eur. Phys. J.* **C22**, 715 (2002).
12. L. G. Landsberg, *Phys. Atom. Nuc.* **68**, 1190 (2005).
13. R. N. Cahn and H. Harari, *Nuc. Phys.* **B176**, 135 (1980).
14. S. Dimopoulos and J. Ellis, *Nucl. Phys.* **B182**, 505 (1981); T. Appelquist, N. Christensen, M. Piai, and R. Shrock, *Phys. Rev* **D70**, 093010 (2004).
15. E. Abouzaid *et al.*, *PRL* **100**, 131803 (2008)
16. K. Arisaka *et al.*, *Phys. Lett* **B432**, 230 (1998).
17. R. Appel *et al.*, *Phys. Rev. Lett.* **85**, 2450 (2000); *Phys. Rev. Lett.* **85**, 2877 (2000).